DOE/ET-53088-193

IFSR #193

SOLITARY VORTICES IN A ROTATING PLASMA

W. Horton, J. Liu, J.D. Meiss, J.E. Sedlak

Institute for Fusion Studies
The University of Texas at Austin
Austin, Texas 78712

May 1985

1 93

SOLITARY VORTICES IN A ROTATING PLASMA

W. Horton, J.Liu, J.D.Meiss, J.E. Sedlak

Institute for Fusion Studies

The University of Texas at Austin. Austin, Texas 78712

ABSTRACT: Nonlinear equations describing the flute dynamics of rotating plasma are derived and solitary vortex solutions are obtained. The solution takes the form of a shielded dipole vortex, similar to that found for nonlinear Rossby waves. The nonlinear dispersion relation, relating propagation speed to vortex radius is obtained. Vortex speeds are shown to take values complementary to the phase velocities of the linear modes of the system. The $\mathbf{E} \times \mathbf{B}$ circulation velocity of the plasma trapped in the vortex is comparable to the diamagnetic drift velocity in the equilibrium plasma.

1.Introduction

The solitary vortex solution obtained by Larichev and Reznik for nonlinear Rossby waves[1] has also been applied to oceanography as a model for gulf stream rings[2,3] and to drift waves[4,5], flute-interchange and other modes[7−12] in a magnetically confined plasma. At the same time, laboratory experiments have confirmed the existence of these vortices in rotating shallow fluids[16−18], numerical experiments have indicated the robustness in strong interactions of the solutions [5,6,19], and linear stability for certain special cases has been proved[20]. Based on these facts it could reasonably be expected that solitary vortices will play as essential a role in two-dimensional fluids as the classical soliton does in the one-dimensional case[10].

In this paper we will show that a low β, inhomogeneous, rotating plasma column immersed in a constant axial magnetic field can exhibit solitary vortex solutions as well. These vortices take the form of a shielded dipole, the vorticity falling off exponentially at large distances. They travel in the azimuthal direction with a constant velocity. We obtain the relation between the velocity, the core size of the vortex dipole,and various system parameters, which we refer to as the nonlinear dispersion relation by analogy with the corresponding relation between linear phase velocity and wavenumber. The nonlinear dispersion relation shows that the velocities of the vortices and the phase speeds of the linear modes occupy complementary regions of parameter space. This complementarity also holds true for most one-dimensional

soliton systems, as well as the other cases for which solitary vortex solutions are known.

The arrangement of this paper as follows: in section 2 we give the derivation of the equations; in section 3, the solitary vortex solution and nonlinear dispersion relation; in section 4, a discussion of the properties of the vortices, and finally in section 5 we give the summary and conclusions.

2.Derivation of Equations

Suppose a dense plasma column is immersed in a constant axial magnetic field $\mathbf{B} = B_o\hat{\mathbf{z}}$. The equilibrium density and electrostatic potential of the plasma are $n_o(\mathbf{x}) = n_o(r)$, $\phi_o(\mathbf{x}) = \phi_o(r)$ respectively (see Fig. 2.1). To imitate the curvature of magnetic field lines which always exists in magnetic confinement devices, we introduce a fictitious gravity

$$\mathrm{g}(r,\theta) = -\nabla U(r,\theta).$$

Taking the ion and electron temperatures as constants , $\nabla T_{i,e} = 0$, the two–fluid macroscopic equations are:

$$\frac{\partial n_j}{\partial t} + \nabla \cdot (n_j \mathbf{v}_j) = 0 \tag{2.1}$$

$$m_j n_j \frac{d\mathbf{v}_j}{dt} = n_j q_j (\mathbf{E} + \frac{1}{c}\mathbf{v}_j \times \mathbf{B}_j) - \nabla p_j - \nabla \cdot \Pi^{(j)} - m_j n_j \nabla U \tag{2.2}$$

$$p_j = n_j T_j \tag{2.3}$$

We treat low-β plasma so we can suppose that the perturbation is electrostatic. We also assume the plasma to be quite dense so instead of the Poisson equation we use the quasineutrality condition

$$\sum_j n_j q_j = 0 \tag{2.4}$$

To close the system of the equations we assume the plasma to be collisionless and that the viscosity tensor Π only to contain gyroviscosity. In the flute approximation the components of this tensor in cylindrical coordinates are:

$$\Pi^{(j)}{}_{rr} = -\Pi^{(j)}{}_{\theta\theta} == -\frac{n_j T_j}{2\omega_{cj}}\left(\frac{\partial v_\theta}{\partial r} - \frac{1}{r}\frac{\partial v_r}{\partial \theta} - \frac{v_\theta}{r}\right)^{(j)}$$

$$\Pi^{(j)}{}_{r\theta} = \Pi^{(j)}{}_{\theta r} = \frac{n_j T_j}{2\omega_{cj}}\left(\frac{\partial v_r}{\partial r} - \frac{1}{r}\frac{\partial v_\theta}{\partial \theta} - \frac{v_r}{r}\right)^{(j)} \tag{2.5}$$

Equations (2.1)-(2.5) are the basic equations describing our system. We now make the following physically reasonable assumptions for simplicity and mathematically tractability:

(a) Neglect electron mass, m_e/m_i=0.

(b) Hydrogen plasma, $q_i = -q_e = e$.

(c) Flute approximation, all physical quantities are z independent.

(d) Low frequency perturbation, the typical frequency of perturbation $\omega \ll$ ion gyrofrequency ω_{ci}.

Under these assumptions, we can reduce the basic equations to a pair of nonlinear equations of the unknown functions n(r,θ,t) and ϕ(r,θ,t)

$$\frac{\partial n}{\partial t} + \frac{c}{B}[\phi, n] = 0 \tag{2.6}$$

$$\frac{c}{B}\frac{1}{\omega_{ci}}\nabla \cdot \{n\frac{\partial}{\partial t}\nabla\phi + \frac{c}{B}n[\phi, \nabla\phi] + \frac{cT_i}{Be}[n, \nabla\phi]\} + \frac{1}{\omega_{ci}}[n, U] = 0 \tag{2.7}$$

where $[f, g] = \hat{\mathbf{z}} \times \nabla f \cdot \nabla g$ is the Poisson bracket or Jacobian. In cylindrical coordinates it can be expressed as

$$[f, g] = \frac{1}{r}(\frac{\partial f}{\partial r}\frac{\partial g}{\partial \theta} - \frac{\partial f}{\partial \theta}\frac{\partial g}{\partial r}).$$

The function $n(r, \theta, t) = n_o(r) + \delta n(r, \theta, t)$ is the number density of the plasma, and $\phi(r, \theta, t) = \phi_o(r) + \delta\phi(r, \theta, t)$ is the electrostatic potential.

The equations (2.6) and (2.7) are, in fact, the electron continuity equation and the quasineutrality condition respectively. Comparing with equations (24) and (25) of Ref.14, it is easy to see that in (2.7) we have included the lowest order FLR effect of the ions through the term $\frac{cT_i}{Be}[n, \nabla\phi]$.

For a closed system one can prove that the nonlinear equations (2.6) and (2.7) conserve the following quantities :

(1) Total number of particles in plasma

$$\frac{d}{dt}\int nrdrd\theta = 0.$$

(2) Total entropy

$$\frac{d}{dt}\int \sum_j S(n_j)rdrd\theta = 0,$$

where $S(n_j) = -n_j \ln (n_j T_j^{\frac{3}{2}}), \quad (j = i, e).$

(3) Total energy

$$\frac{d}{dt}\int nm_i[\frac{(\nabla\phi)^2}{2} + U]rdrd\theta = 0.$$

(4) Total angular momentum

$$\frac{d}{dt}\int rnv_\theta rdrd\theta = \int nrF_\theta rdrd\theta,$$

where $v_\theta = \frac{c}{B}\frac{\partial\phi}{\partial r}, F_\theta = -\frac{1}{r}\frac{\partial U}{\partial\theta}$. Usually we take $U = U(r)$, so $F_\theta = 0$, the angular momentum is conserved. In the expressions of energy and angular momentum we neglect the contribution of the electron component since $m_e/m_i \sim 0$.

If the equilibrium $\mathbf{E} \times \mathbf{B}$ drift of the plasma column is a uniform rotation about the $\hat{\mathbf{z}}$ axis, then

$$\phi_o(r) = \frac{B\Omega}{2c}r^2 + constant, \tag{2.8}$$

where the plasma rotation frequency Ω=constant.

Transforming the equations (2.6) (2.7) into the rotating frame yields

$$\frac{\partial \delta n}{\partial t} + \frac{c}{B}[\delta\phi, n] = 0 \tag{2.9}$$

$$\frac{c}{B\omega_{ci}}\nabla\cdot\{n\frac{\partial}{\partial t}\nabla\delta\phi + \frac{c}{B}n[\delta\phi,\nabla\delta\phi] + \frac{cT_i}{Be}[n,\nabla\delta\phi]\} - \frac{2c\Omega}{B\omega_{ci}}[n,\delta\phi]$$

$$+\frac{1}{\omega_{ci}}[n, U - \frac{r^2\Omega^2}{2}] = 0. \tag{2.10}$$

The linear global mode analysis of (2.9) and (2.10) was reported in Ref.13 (for $T_i = 0$) and Refs.12,14 (for $T_i \neq 0$) for specific equilibrium density and potential profiles. Their results showed that when the azimuthal wave mode number is small, m$\leq$3, the modes are quite global, but when m$\geq$ 4 the linear modes are basically localized around the edge of the plasma column [see Fig.2.2]. The linear analysis also shows that for low ion temperature $T_i < T_e$, i.e.the ion FLR effect is not very strong, then the high m modes have much higher growth rate than low m global modes. Based on those results we propose that the nonlinear interaction between the local high m modes at the plasma edge is dominant at a certain stage of the nonlinear evolution. During this stage, we can suppose the characteristic length of the perturbed density and potential is small, i.e.

$$|\frac{d\ln\delta n}{dr}|^{-1}, |\frac{d\ln\delta\phi}{dr}|^{-1} \ll r_n = |\frac{d\ln n_o}{dr}|^{-1}.$$

In this case, equations (2.9) and (2.10) reduce to

$$\frac{\partial\tilde{n}}{\partial t} - \frac{cT_e}{Be}\frac{1}{n_o}\frac{\partial n_o}{\partial r}\frac{\partial\tilde{\phi}}{r\partial\theta} = \frac{cT_e}{Be}[\tilde{n},\tilde{\phi}] \tag{2.11}$$

$$\frac{1}{\omega_{ci}}\frac{cT_e}{Be}(\frac{\partial}{\partial t}+\frac{T_i}{m_i\omega_{ci}}\frac{1}{n_o}\frac{\partial n_o}{\partial r}\frac{\partial}{r\partial\theta})\nabla^2\tilde{\phi}-2\frac{\Omega}{\omega_{ci}}\frac{cT_e}{Be}\frac{1}{n_o}\frac{\partial n_o}{\partial r}\frac{\partial\tilde{\phi}}{r\partial\theta}$$
$$+\frac{1}{\omega_{ci}}(\Omega^2 r+g(r))\frac{\partial\tilde{n}}{r\partial\theta}=\frac{1}{{\omega_{ci}}^2}\frac{{cT_e}^2}{Bem_i}[\nabla^2\tilde{\phi},\tilde{\phi}+\frac{T_i}{T_e}\tilde{n}] \qquad (2.12)$$

where $\tilde{n}=\frac{\delta n}{n_o(r)}$, $\tilde{\phi}=\frac{e\delta\phi}{T_e}$.

Since the small-sized perturbations are localized around the edge of the plasma the cylindrical geometry of the configuration is less important, and we can use Cartesian coordinates:

$$\frac{r}{r_n}\longrightarrow x$$
$$\frac{r\theta}{r_n}\longrightarrow y.$$

Using a dimensionless time τ,

$$t\frac{\rho_s v_s}{{r_n}^2}\longrightarrow\tau,$$

equations (2.11), (2.12) become

$$\frac{\partial\tilde{n}}{\partial\tau}+\frac{\partial\tilde{\phi}}{\partial y}=[\tilde{n},\tilde{\phi}] \qquad (2.13)$$

$$(\frac{\partial}{\partial\tau}-\frac{T_i}{T_e}\frac{\partial}{\partial y})\nabla^2\tilde{\phi}+v_c\frac{\partial\tilde{\phi}}{\partial y}+v_g\frac{\partial\tilde{n}}{\partial y}=[\nabla^2\tilde{\phi},\tilde{\phi}+\frac{T_i}{T_e}\tilde{n}] \qquad (2.14)$$

where

$$v_c=\frac{2\Omega}{\frac{\rho_s v_s}{{r_n}^2}}=2\hat{\Omega}$$

$$v_g=(\frac{r_n}{\rho_s})^2(\frac{\Omega^2 r_n r}{{v_s}^2}+\frac{r_n g(r)}{{v_s}^2})=\hat{\Omega}^2 r/r_n+\hat{g}$$

v_c is Coriolis drift, v_g represents the centrifugal and gravitational drift. We take the localized value of v_g as constant in further calculations. Also

$$v_s = (\frac{T_e}{m_i})^{\frac{1}{2}}, \qquad \rho_s = \frac{v_s}{\omega_{ci}}.$$

The equations (2.13) and (2.14) are the nonlinear equations for which we seek the solitary vortex solution. Before proceeding to the solution it might be worthwhile to mention that:

(i) Equation (2.13) and (2.14) are very similar to the equations derived by Rahman and Weiland[21] for high β plasma, except for the second term of (2.14)which comes from the Coriolis force in the rotating frame. Heuristically, since plasma in toroidal devices experiences poloidal rotation in certain situation, the analysis of our problem may give some insight into that case as well.

(ii) Compared with the equations given by Pavlenko and Petviashivili [7], our equations differ from theirs by two terms: the first one is the Coriolis term intrinsic to the rotating frame while the second one is the second nonlinear term in equation (2.14) which they missed by error as pointed out by Mikhailovskii et al[10].

3. Solitary Vortex

We seek a stationary solution of (2.13) and (2.14) in the form of

$$\tilde{n}(x,y,t) = \tilde{n}(x,y')$$

$$\tilde{\phi}(x,y,t) = \tilde{\phi}(x,y') \tag{3.1}$$

where $y' = y - u\tau$, u=const. is a free parameter.

Substituting (3.1) into (2.13), (2.14), we have

$$\frac{\partial}{\partial y'}(\tilde{\phi} - u\tilde{n}) = [\tilde{n}, \tilde{\phi}] \tag{3.2}$$

$$-(u + \frac{T_i}{T_e})\frac{\partial}{\partial y'}\nabla^2\tilde{\phi} + v_c\frac{\partial\tilde{\phi}}{\partial y'} + v_g\frac{\partial\tilde{n}}{\partial y'} = [\nabla^2\tilde{\phi}, \tilde{\phi} + \frac{T_i}{T_e}\tilde{n}]. \tag{3.3}$$

In the remainder of this paper we drop the tildes on n and ϕ for convenience.

To solve (3.2), (3.3), we divide the $x - y'$ plane into two regions

$$\textbf{Region I} : x^2 + y'^2 < {r_o}^2$$

$$\textbf{Region II} : x^2 + y'^2 > {r_o}^2$$

where r_o is a constant parameter characterizing the size of the vortex. We look for solutions which satisfy the following conditions:

(1) In Region I, n and ϕ must be finite at $r = (x^2 + y'^2)^{\frac{1}{2}} = 0$.

(2) In Region II, when $r \to \infty$, n and ϕ must decay to zero.

(3) On the border between Region I and Region II, where $r = r_o$:

(a) The stream function must be continuous, $(\phi)_I = (\phi)_{II}$.

(b) The velocity field must be continuous, $\hat{\mathbf{z}} \times (\nabla\phi)_I = \hat{\mathbf{z}} \times (\nabla\phi)_{II}$.

(c) The vorticity must be continuous, $(\nabla^2\phi)_I = (\nabla^2\phi)_{II}$.

(d) The density perturbation must be continuous, $(n)_I = (n)_{II}$, where subscripts I, II denote the corresponding quantities in Region I and Region II.

After some algebra we find that to satisfy conditions (1),(2), the simplest solutions n, ϕ should satisfy following equations

In Region I ($r < r_o$)

$$n = d\phi + (1 - du)x \tag{3.4}$$

$$\nabla^2\phi = -p^2\phi + Cx \tag{3.5}$$

$$C = (v_c + dv_g) + p^2 u \tag{3.6}$$

In Region II ($r > r_o$)

$$n = \frac{\phi}{u} \tag{3.7}$$

$$\nabla^2\phi = k^2\phi \tag{3.8}$$

$$k^2 = \frac{v_c u + v_g}{u(u + T_i/T_e)}. \tag{3.9}.$$

Here k,p,d and C also are real constants related by equations (3.6),(3.9).

Solving equations (3.4)-(3.9), and imposing the matching conditions 3(a),(b),(c),(d), we obtain the solutions

$$\phi = \begin{cases} [-\frac{k^2 r_o}{p^2 r}\frac{J_1(pr)}{J_1(pr_o)} + (1+\frac{k^2}{p^2})]ur\cos\theta & (r < r_o) \\ ur_o\frac{K_1(kr)}{K_1(kr_o)}\cos\theta & (r > r_o) \end{cases} \tag{3.10}$$

$$n = \begin{cases} [\frac{k^2}{p^2}\frac{u(uk^2 - v_c)}{v_g}(1 - \frac{r_o J_1(pr)}{rJ_1(pr_o)}) + 1]r\cos\theta & (r < r_o) \\ \frac{K_1(kr)}{K_1(kr_o)}r_o\cos\theta & (r > r_o) \end{cases} \tag{3.11}$$

where $\theta = \tan^{-1}\frac{y\prime}{x}$, k is real parameter defined by (3.9). Parameters k and p are related by

$$\frac{1}{kr_o}\frac{K_2(kr_o)}{K_1(kr_o)} = -\frac{1}{pr_o}\frac{J_2(pr_o)}{J_1(pr_o)} \tag{3.12}$$

where J and K are Bessel and McDonald functions.

From (3.10)-(3.12) we can see that both n and ϕ have the form of a vortex pair moving with constant velocity u in the y direction,i.e. in the azimuthal direction around the edge of the plasma column. The radial size of the core of each vortex is characterized by parameter r_o, and the strength is a complicated function of two independent free parameters u and r_o. In the exterior region ($r > r_o$) the vortices decay to zero as $e^{-kr}/r^{\frac{1}{2}}$.

4. Properties of the Vortices

In this section we consider (1) the nonlinear dispersion relation, (2) the bounds of propagation speeds, (3) the complementary phase velocities of the linear modes, and (4) spatial structure of the vortex flows.

(1) Nonlinear dispersion relation

The vortices derived in section 3 are a two parameter family of exact solutions to the field equations. The free parameters are taken either as the core size r_o and speed u, or the core size r_o and exterior scale size k. Equation (3.9) relates the two alternative choices of parameters speed u or exterior scale size k, conventionally we call it nonlinear dispersion relation. The requirement that the vortices decay to zero in the exterior region constraints the speed u of the vortices to be within the bounds determined by $k^2(u) > 0$, i.e.

$$k^2 = \frac{uv_c + v_g}{u(u + T_i/T_e)} > 0. \tag{4.1}$$

For this reason we find it more convenient to parameterize the vortices as shown in Fig.4.1 with the core size r_o and exterior decay rate k.

The vortices are computed by specifying the plasma parameters $\Omega, g, T_i/T_e$ and the vortex parameters r_o, k. The relation (3.12)which relates p with k is solved for the principal branch of $pr_o = f(kr_o)$ defined by $\gamma_1 \leq pr_o \leq \gamma_2$ where γ_1 is the first nonzero root of $J_1(x)$ and γ_2 is the first root of $J_2(x)$. For each k the two branches of the solutions of equation (4.1) for vortex velocities $u_\pm(k^2, T_i/T_e, v_c, v_g)$

are computed and then the vortex fields (3.10) and (3.11) are determined.

(2) Propagation speeds of the vortices

The vortices can only propagate in certain bands of speeds that are determined by the plasma parameters Ω, g and T_i/T_e.

The limits on the vortex propagation bands are determined by inequality (4.1) which is equivalent to the inequalities

$$uv_c + v_g > 0 \quad and \quad u(u + \frac{T_i}{T_e}) > 0 \tag{4.2}$$

or

$$uv_c + v_g < 0 \quad and \quad u(u + \frac{T_i}{T_e}) < 0 \tag{4.3}$$

For different directions of plasma rotation the conditions (4.2) and (4.3) give different propagation bands which are shown in Fig.4.2.

(i) Inward equilibrium electric field

For radially inward equilibrium electric fields ($\Omega > 0$), zero or bad curvature $v_c > 0$ and $v_g > 0$. The regions of vortex propagation are

$$u > 0 \tag{4.4}$$

and

$$-\frac{T_i}{T_e} > u > -\frac{v_g}{v_c}, \quad if \quad \frac{T_i}{T_e} < \frac{v_g}{v_c} \tag{4.5}$$

or

$$-\frac{v_g}{v_c} > u > -\frac{T_i}{T_e}, \quad if \quad \frac{T_i}{T_e} > \frac{v_g}{v_c} \tag{4.6}$$

(ii) Outward equilibrium electric field

For radially outward equilibrium electric fields ($\Omega < 0$)and bad curvature $v_c < 0, v_g > 0$,the vortex propagation bands are

$$-\frac{v_g}{v_c} > u > 0 \tag{4.7}$$

and

$$u < -\frac{T_i}{T_e} \tag{4.8}$$

From equations (4.4–4.8) we see that there is wide region of propagation in the direction of the plasma rotation, but only a limited region in which the vortices may travel in the opposite direction. This behavior of the plasma vortices is similar to the situation observed in the rotating shallow fluid experiments[16–18].

(3)**Complementary regions of linear modes**

In the gaps where vortices do not propagate, the linear wave modes of the system propagate with the phase velocity $u_p = \omega/(k_y V_{de}) = r\omega/(mV_{de})$.

Returning to the field equations (2.13) and (2.14) and looking for the linear modes in form of $e^{(ik_x x + ik_y y - i\omega t)}$, we obtain the dispersion relation

$$k_\perp^2 c_p(c_p + T_i/T_e) + v_c c_p + v_g = 0 \tag{4.9}$$

where $c_p = \omega/(k_y V_{de})$ and $k_\perp^2 = k_x^2 + k_y^2 > 0$. Alternatively, one may return to the full radial equations (2.11) and (2.12) and solve for the eigenmodes $\phi_m(r)e^{(im\theta - i\omega t)}$

for the rigid rotor equilibrium. In this case one also obtains equation (4.9) with $c_p = a\omega/(mV_{de}), k_\perp^2 \rightarrow \nu(m,n,b/a)$ where $\nu_{m,n}$ are eigenvalues of second order differential equation $y''+(\frac{1}{x}-x)y'+(\nu-m^2/x^2)y = 0$ with the boundary conditions $y(0) = y(b/a) = 0$, where a,b are geometric parameters of the rigid rotor equilibrium [for details see Refs.14-15]. The eigenvalues $\nu_{m,n}$ are discrete and positive definite so that in this case the phase velocities c_p lie in the continuum between the vortex propagation bands. Thus, equations (4.1) for the vortices and (4.9) for the waves cover all values of external wave number or decay scale as shown in Figs. 4.2.

The wave dispersion relation (4.9) predicts exponential growth for parameters $\Omega, g, T_i/T_e$ which make a negative discriminant $B^2 - 4AC < 0$ for the quadratic equation $Ac_p^2 + Bc_p + C = 0$, where $A = {k_\perp}^2, B = {k_\perp}^2 T_i/T_e + v_c, C = v_g$. In the unstable parameter region the phase velocity is $c_p = -B/2A$. The unstable regions are analyzed in details in Refs.14-15.

(4) **Spatial structure of the vortices**

We now consider the variation in the vortex fields with the vortex parameters. We show that the vortices propagating in the electron or ion diamagnetic direction have different behavior (for convenience we call them electron or ion diamagnetic vortex respectively). The ion diamagnetic vortex requires considerably larger energy for excitation than the electron diamagnetic one for comparable vortex parameters r_o and k.

As a reference system we consider a plasma column rotating in the ion diamag-

netic direction with a speed twice the ion diamagnetic speed, $\hat{g} = 1$, and a core size 1/5 the density gradient scale length r_n with $T_i = T_e = T$. The speed of propagation of the two branches is shown in Fig. 4.3. For comparison, we also give a similar Fig. 4.4 for a plasma column rotating in electron diamagnetic direction with the same speed.

For vortices with external scale sizes, 1/k, comparable to the density gradient scale length r_n, the speeds of propagation are large compared with the diamagnetic drift speeds. Strictly speaking, due to the conditions we gave in the derivation of equations (2.11) and (2.12), our analytic solutions are not appliable for these large vortices.

For vortices with small external scale sizes compared to r_n, the speeds of propagation are close to those of the linear modes of the system. At large k the speeds approach the limiting speeds as $1/k^2$.

In Figs.4.5 and 4.6 we show the variation of the electron and ion diamagnetic vortex fields with k for the reference parameters used in Fig.4.3.

The electron diamagnetic vortex has a maximum of the electrostatic potential at $r \simeq r_o/2$ with $e\phi_{max}/T \simeq 2.3 r_o/k$ for $k = k_\perp r_n > 1$. This maximum of the potential is consistent with the mixing length for modes for $\mathbf{E} \times \mathbf{B}$ convective saturation, $V_E \simeq V_{de}$ or $e\phi/T_e \approx 1/(k_x r_n)$, which we know to apply to drift waves and their turbulent spectra.

The ion diamagnetic vortices have larger electrostatic fields than the electron

diamagnetic vortices for comparable r_o and k as shown by the comparison of Fig. 4.6 and 4.5. The electrostatic potentials have maxima at roughly $|e\phi_{max}/T_e| \simeq 12r_o/k$, and thus have $|e\phi_{max}| > T_e$ for $k = k_\perp r_n \leq 12r_o$. The energy required to excite the ion vortex is large. The polarization of the ion vortex is characteristic of MHD motions with $|e\phi/T| \gg |\delta n/n|$. As the exterior scale of the ion vortex decreases, the maximum potential decreases until reaching a minimum value $|e\phi_{min}/T| \simeq 2$ or $3r_o$. The value of k at which this minimum occurs decreases from $k \simeq 14.5$ for $r_o = .05$ to $k \simeq 6.5$ for $r_o = 0.3$. The saturation of ϕ at ϕ_{min} implies that there is minimum excitation energy E_{min} for creation of an ion diamagnetic vortex.

5. Summary and Conclusions

In summary, in this work we have derived the nonlinear equations describing flute dynamics of low frequency electrostatic perturbations for low β, rotating plasma in crossed electric and magnetic fields. For a closed system this set of equations guarantees the conservation of the total number of particles, total energy and total angular momentum of the rotating plasma column. We obtained localized solutions of the equations corresponding to solitary dipolar vortices. We discussed the nonlinear dispersion relation, the allowed regions of propagation speeds, the structure of the vortices, and the complementary regions of linear modes.

The vortex solutions given here describe the convection of density and vorticity of background plasma on space scales small compared with the radius of the plasma

column. The electron motion in these vortex solutions is flute-like compared with those given earlier in Refs.4-5 which considered adiabatic electrons ($k_{\|}v_e > k_{\perp}u$). A principal difference is that for the drift wave vortex the electron diamagnetic drift velocity v_{de} determines the speed of propagation, whereas for the dipolar vortex it is the Coriolis force $2m_j\mathbf{V}\times\mathbf{\Omega}$ and the finite ion Larmor radius drift velocity that determine the speed of propagation of the vortex. For small ion-to-electron tempetrature ratios the speed of propagation in the direction of plasma rotation is given approximately by $u = 2\Omega/k_{\perp}^2 r_n$.

The dominant direction of flute vortex propagation is in the direction of the plasma rotation although counter streaming solutions also occur.

We show that the scale of the maximum potential ϕ_m in the vortex scales as $e\phi_m/T \sim 1/(k_{\perp}r_n)$ consistent with the usual estimate for nonlinear $\mathbf{E}\times\mathbf{B}$ convective motion in an inhomogeneous plasma. We show that vortices propagating in the ion diamagnetic direction have a larger maximum potential (by a factor $\simeq 5$) and a much larger vorticity than those propagating in the electron diamagnetic direction. The difference in the strength of the vorticity arises from the partial cancellation of the convective derivative proportional to $u + T_i/T_e$ for the ion diamagnetic vortices.

We note that monopolar vortices of the form $K_o(k_{\perp}r)$ with $r = (x^2 + y'^2)^{1/2}$ are not exact solutions of the equations as the dipole vortices are. A monopolar vortex[19] may occur either as a transient structure decaying in time due to coupling to the wave components of the fields or may be driven by externally imposed sheared

rotation.

Finally, we remark that although the nature of the vortex-wave interaction dynamics remains to be investigated theoretically, the experimental evidence from Refs.16-18 as well as the computer simulations in Refs.5,6,19 show the importance of the interactions between these two components of the field. A vortex with its four parameters x_o, y_o, (initial position of the vortex core) amplitude and speed contain an infinite spectrum of coherent $\mathbf{k}$ modes. We suggest that a theoretical description based on field containing both vortices and wave modes may be more nearly diagonal than a pure modal description.

Acknowledgements

This work is supported by USDOE grant number DE-FGOS-80ET 53088. W.H and J.D.M wish to acknowledge useful discussions with N.J. Zabusky and the hospitality of the Institute for Theoretical Physics, University of Califonia, Santa Barbara.

References

1. V.D. Larichev and G.M. Reznik, Dokl. Akad. Nauk.SSSR **231** 1077 (1976).
2. M.E.Stern, J. Mar. Res. **33** 1 (1975).
3. G.R.Flierl, V.D. Larichev, J.C.McWilliams, and G.M. Reznik, Dyn.Atmos.and Oceans **5** 1(1980).
4. J.D.Meiss and W.Horton, Phys. of Fluids **26** 990 (1983).
5. M.Makino, T.Kamimura and T.Taniuti, J.Phys.Soc.Jap. **50** 980 (1981).
6. J.C.McWilliams and N.J.Zabusky, Geophys. Astrophys.Fluid Dynamics **19** 207(1982)
7. V.P.Pavlenko and V.I.Petviashivili, Soviet Plasma Phys.**9** 603 (1983).
8. A.B.Mikhailovskii,G.D.Aburdzheniya,O.G. Onishchenko,and S.E.Sharapov, Phys.Letters**100A**503 **104A** 94 (1984) A.B.Mikhailovskii, G.D.Aburzheniya, O.G.Onishchenko,and A.P.Churikov,Phys.Letter**101A** 263 (1984).
9. V.I.Petviashivili and V.Pogutse, JETP lett.**39** 436 (1984).
10. A.B. Mikhailovskii,V.P.Lakhin, L.A. Mikhailovskaya,and O.G. Onishchenko, JETP **86** 2061 (1984) (in Russian).
11. P.K.Shukla,K.H.Spatschek, and R.Balescu, Phys.Letter **107A** 461 (1985).
12. R.D.Hazeltine,D.D.Holm ,and P.J.Morrison, IFSR 173 (1985).
13. M.N.Rosenbluth and A.Simon, Phys.of Fluids **10** 1077 (1967).
14. W.Horton and J.Liu, Phys.of Fluids **27** 2067(1984).

15. J.Liu,J.E.Sedlak and W.Horton, Bull.of APS **28** 1407 (1984).

16. C.V.Antipov, M.V.Nezlin, E.N.Snezhkin, and A.S.Trubnikov, JETP **55** 85 (1982). JETP **57** 786 (1983).

17. G.R.Flierl,M.E.Stern,and J.A.Whitehead, Dyn. Atmos. and Oceans **7** 233 (1983).

18. R.A.Antonova, V.P.Zhvaniya, D.G.Lominadze, D.I.Nanobashivili, and V.I.Petviashivili, JETP Lett.**37** 786 (1983).

19. N.J.Zabusky and J.C.McWilliams,Phys. of Fluids **25** 2175 (1982).

20. E.M.Laedke and K.H.Spatschek, Phys. of Fluids **28** 1008 (1985).

21. H.U.Rahman and J.Weiland, Phys.Rev.A **28** 1678 (1982).

Figure Captions

2.1 (a) Configuration of magnetic field and equilibrium electric field in a plasma column. (b) Equilibrium density and electrostatic potential profile of plasma.

2.2 Radial function of electrostatic perturbation for Gaussian density profile $n(r) = n_o e^{-r^2/a^2}$ and solid body rotation, where m is the azimuthal mode number, and b is the location of conducting wall. (a) small b/a, (b) large b/a.

4.1 Schematic diagram of the parameter representation of the vortices.

4.2 Propagation regions of vortices and linear wave modes. Vortices occur in the unhatched regions, and wave modes occur in the hatched regions of the parameter space. The boundary curves are $u = -v_g/v_c$, $u = -T_i/T_e$, and $u = 0$.

4.3 The vortex propagation speed versus inverse external scale size for $\hat{\Omega} < 0$, $T_i/T_e = 1$, $\hat{g} = 1$, and $r_o/r_n = 1/5$.

4.4 The vortex propagation speed versus inverse external scale size for $\hat{\Omega} > 0$; other parameters are the same as Fig.4.3.

4.5 The radial structure of electron diamagnetic vortices ($u > 0$): (a) potential, (b) electric field, (c) vorticity. (The parameters are the same as Fig.4.3.)

4.6 The radial structure of ion diamagnetic vortices ($u < 0$): (a) potential, (b) electric field, (c) vorticity. (The parameters are the same as Fig.4.3.)

(a)

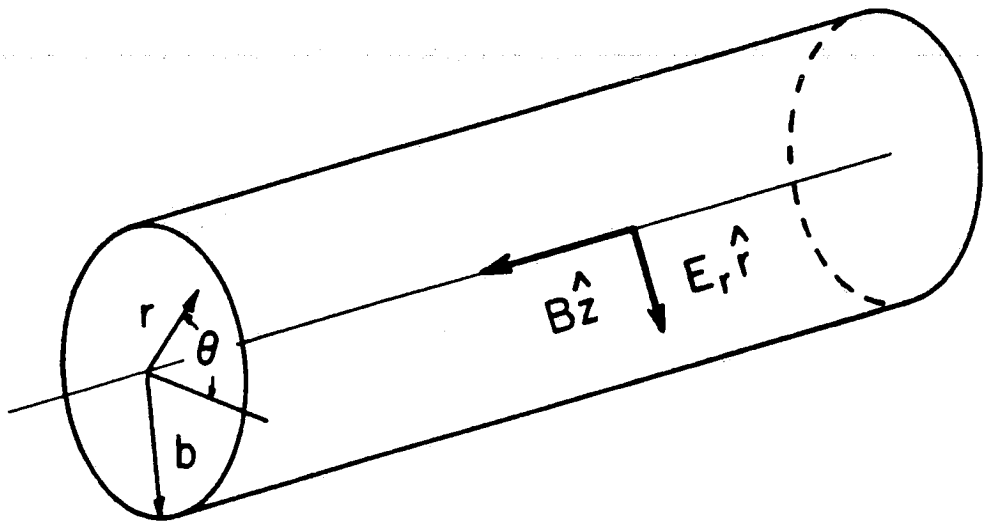

(b)

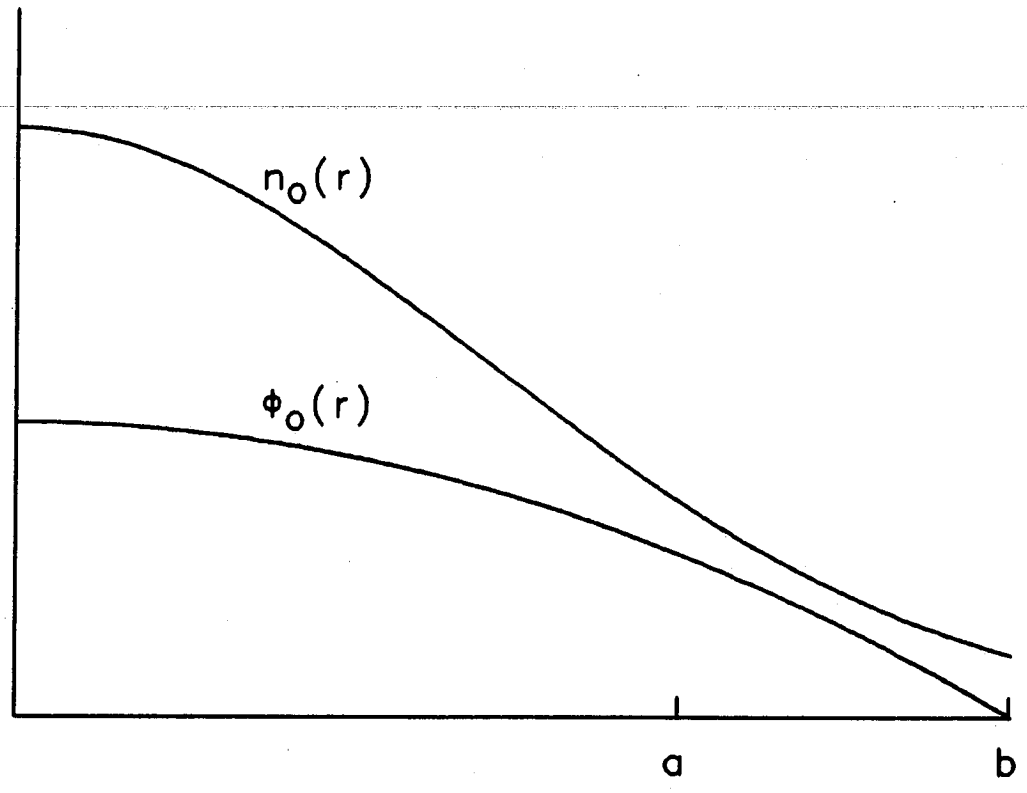

Fig. 2.1

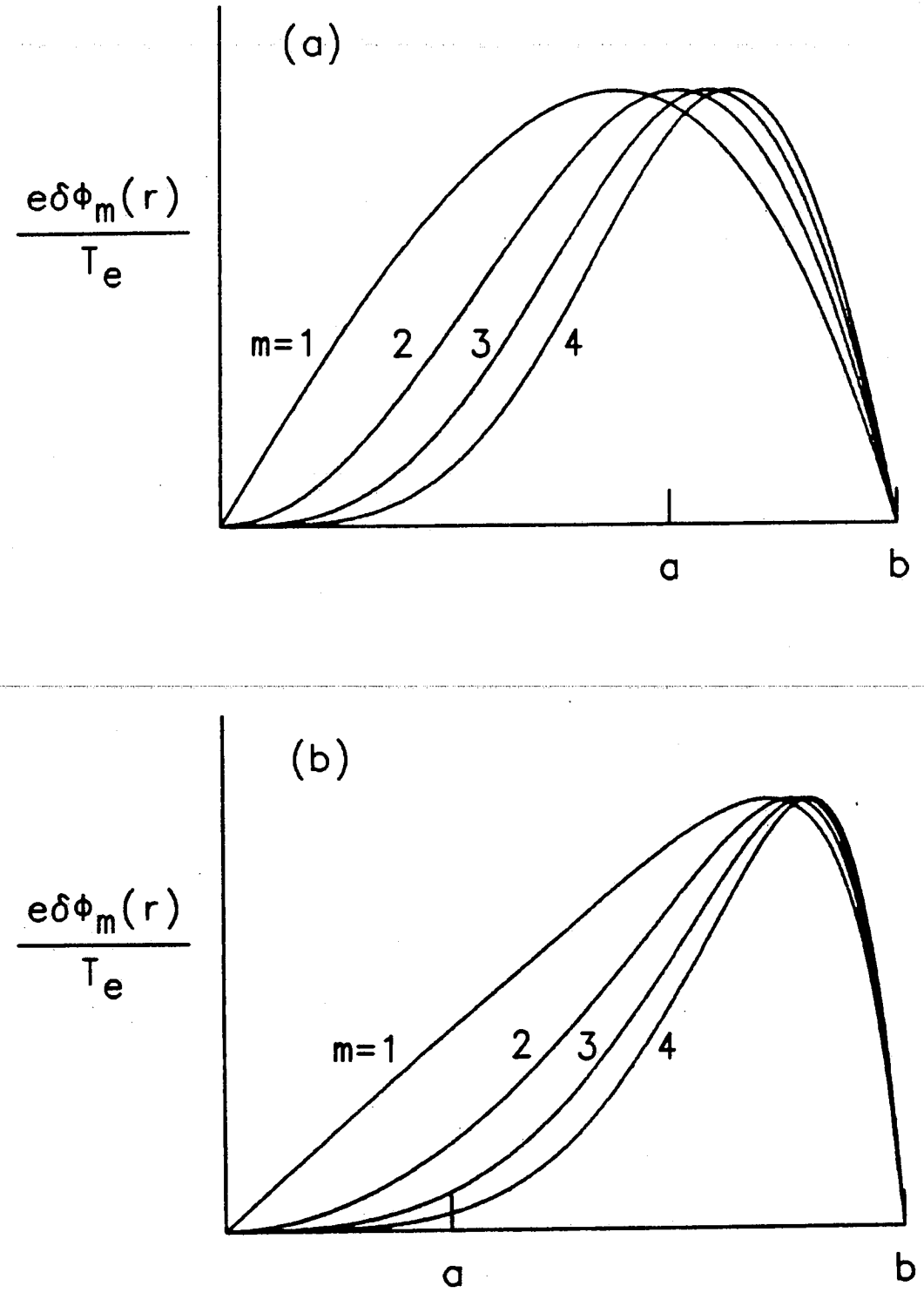
(a)
$\frac{e\delta\Phi_m(r)}{T_e}$
m=1
2
3
4
a
b
(b)
$\frac{e\delta\Phi_m(r)}{T_e}$
m=1
2
3
4
a
b

Fig. 2.2

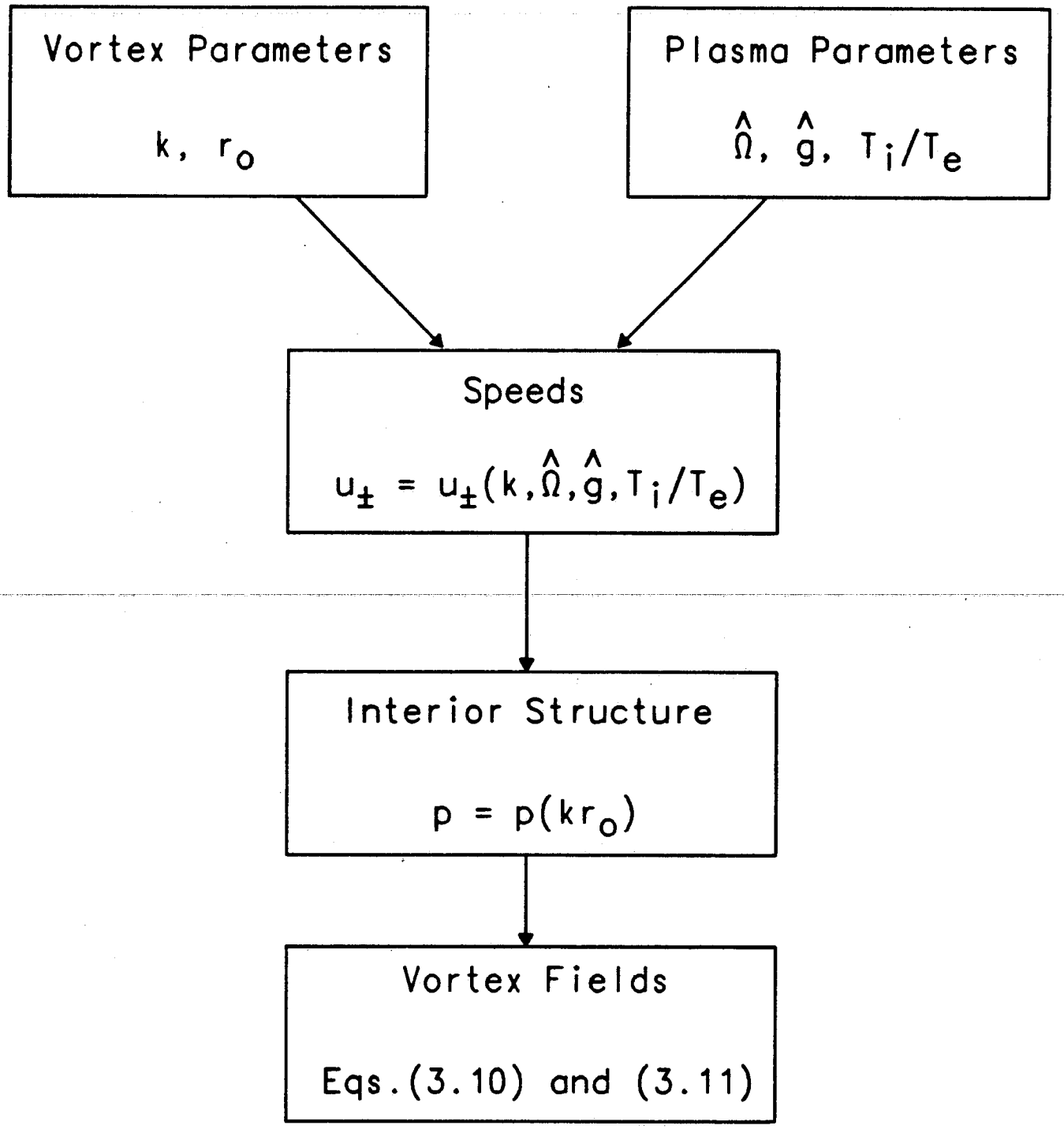
Vortex Parameters
k, r_o
Plasma Parameters
$\hat{\Omega}$, $\hat{g}$, T_i/T_e
Speeds
$u_\pm = u_\pm(k, \hat{\Omega}, \hat{g}, T_i/T_e)$
Interior Structure
$p = p(kr_o)$
Vortex Fields
Eqs.(3.10) and (3.11)

Fig. 4.1

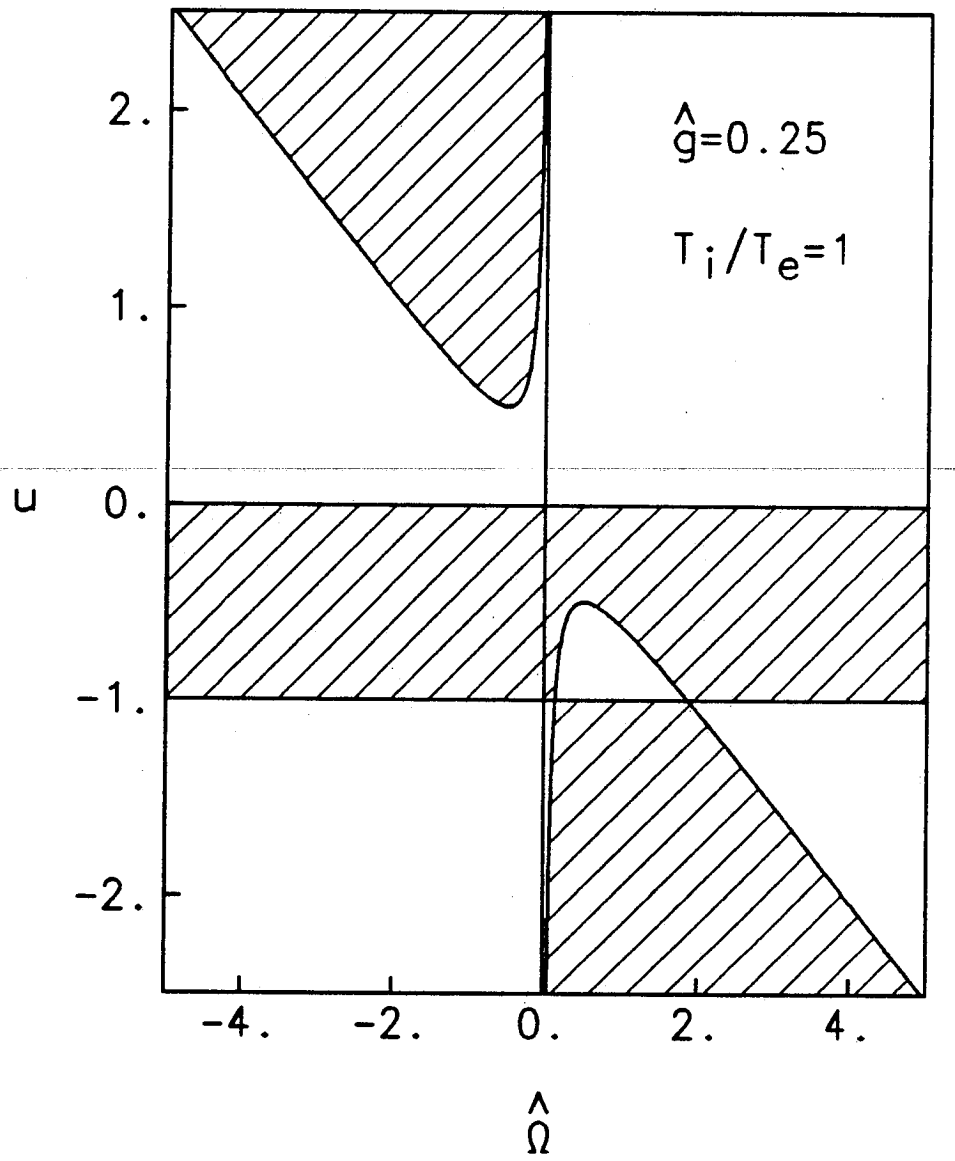

Fig. 4.2

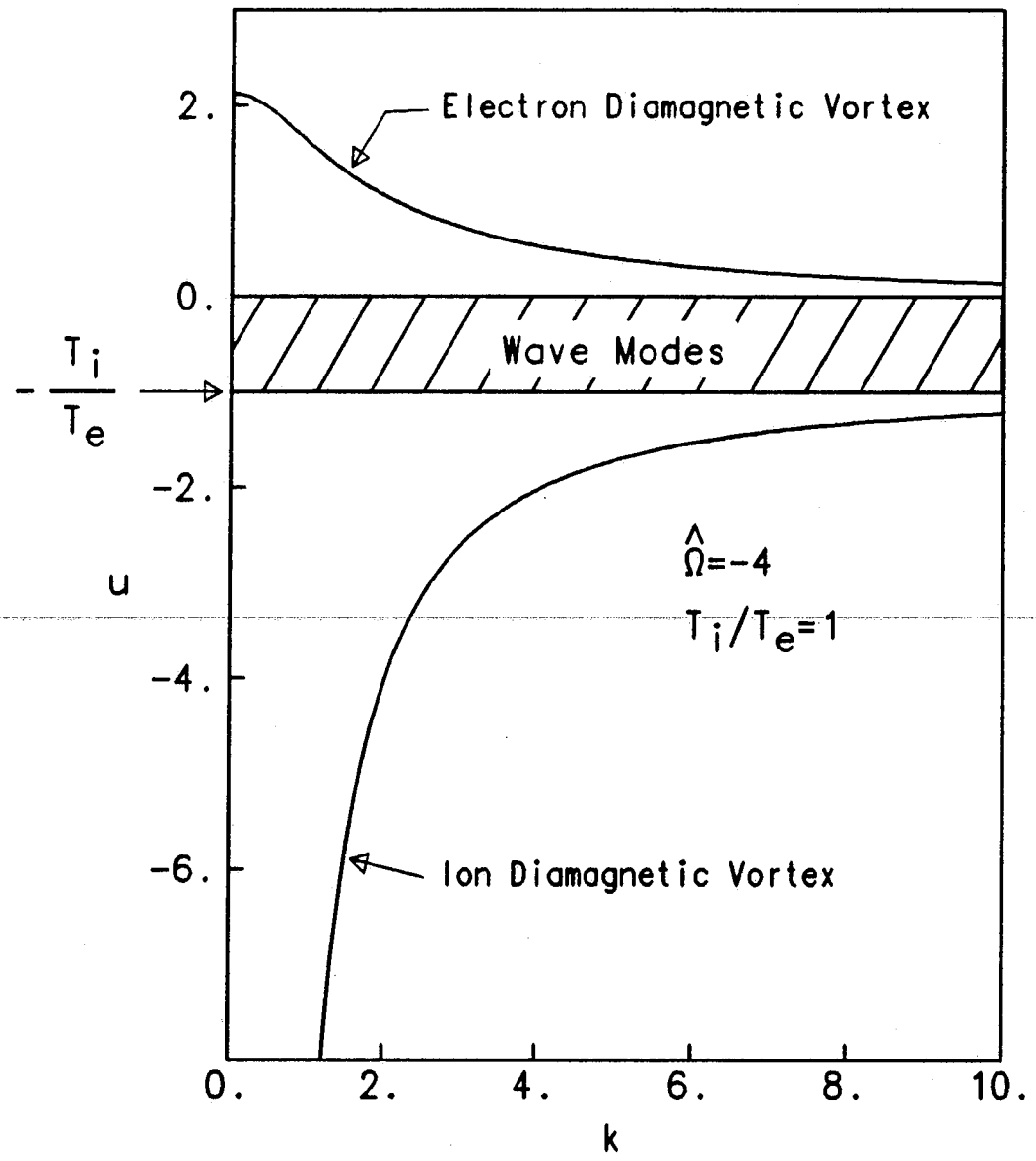
2.
0.
$-\frac{T_i}{T_e}$
-2.
-4.
-6.
u
Electron Diamagnetic Vortex
Wave Modes
$\hat{\Omega}=-4$
$T_i/T_e=1$
Ion Diamagnetic Vortex
0.
2.
4.
6.
8.
10.
k

Fig. 4.3

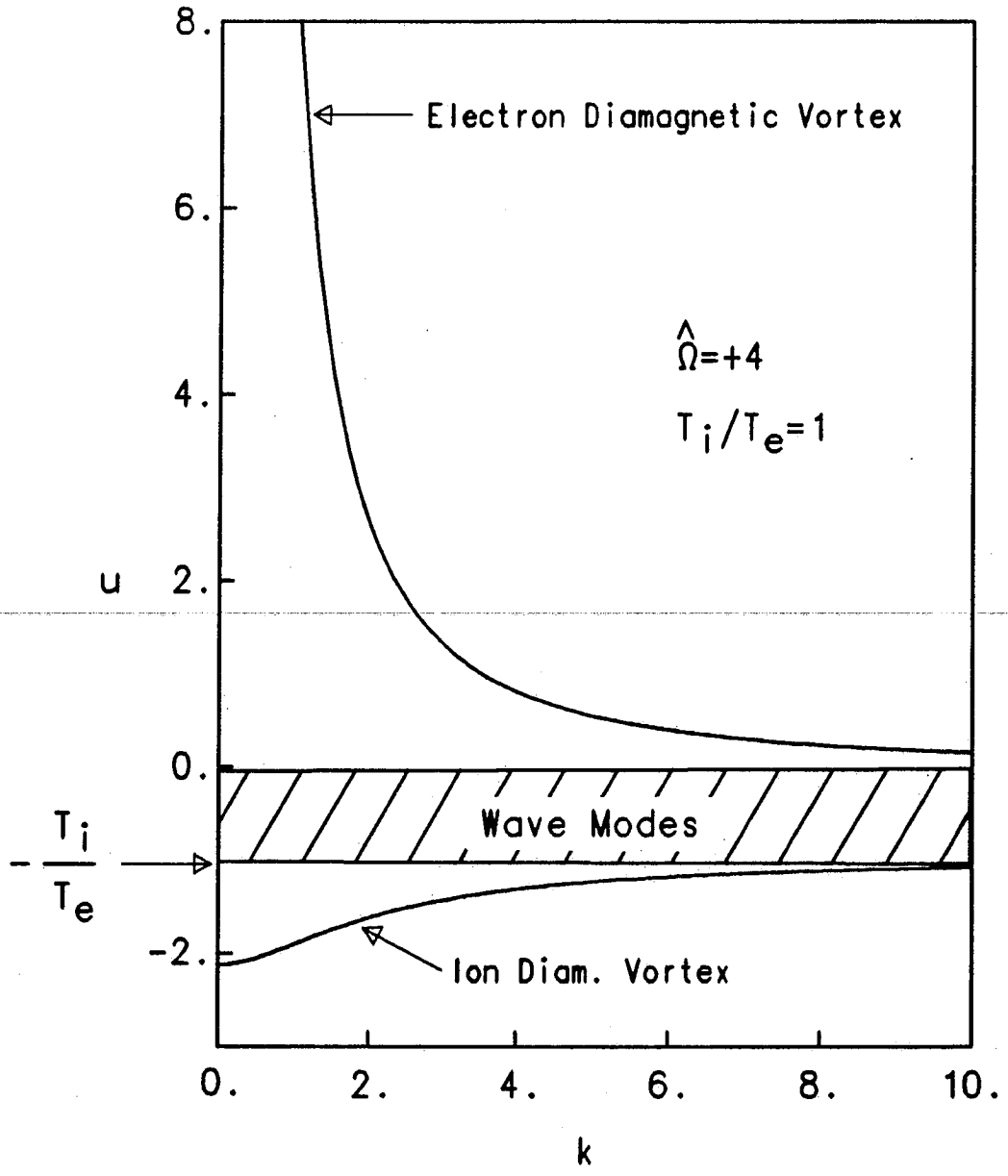
8.
6.
4.
2.
0.
-2.
u
Electron Diamagnetic Vortex
$\hat{\Omega}$=+4
T_i/T_e=1
Wave Modes
$-\frac{T_i}{T_e}$
Ion Diam. Vortex
0.
2.
4.
6.
8.
10.
k

Fig. 4.4

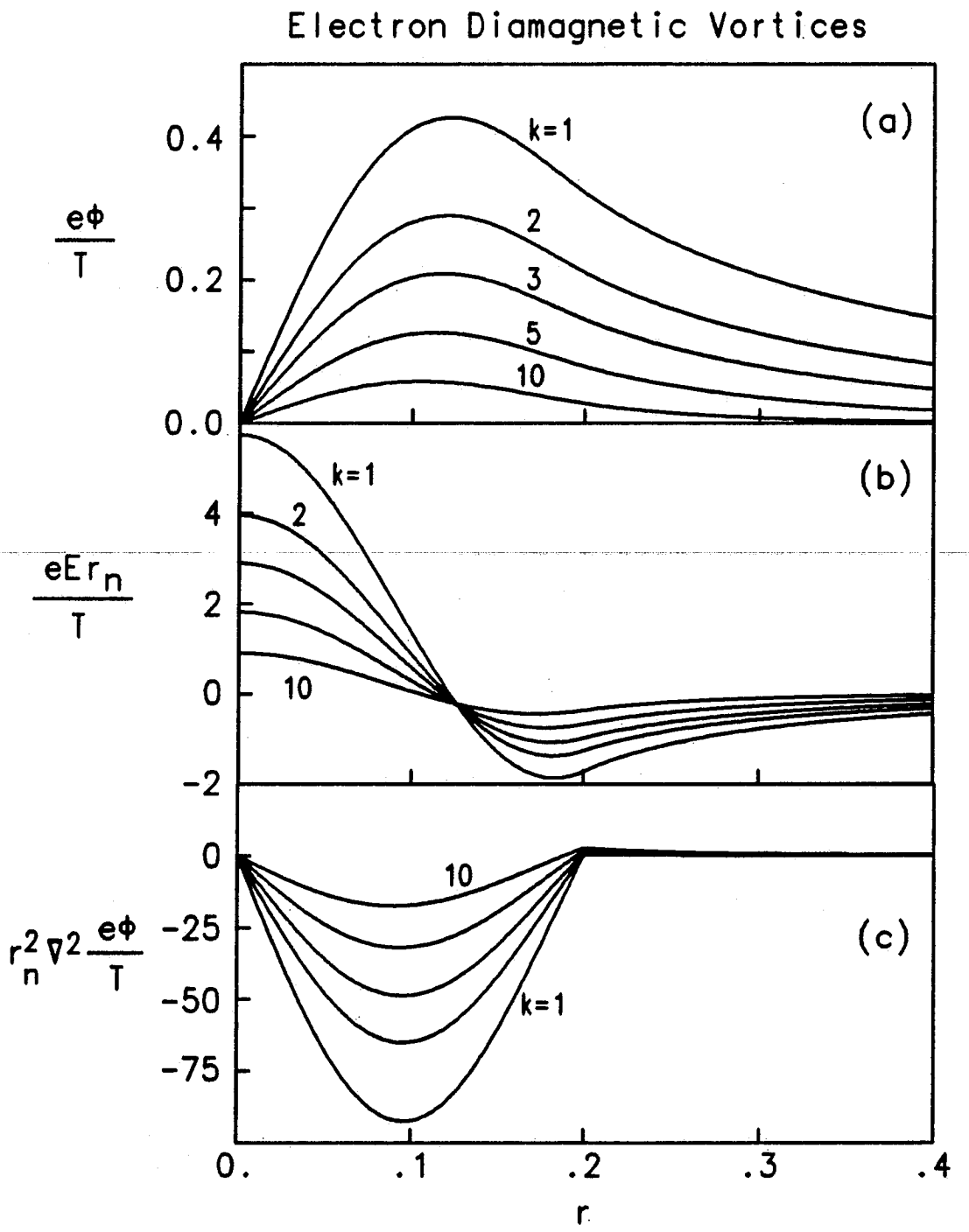
Electron Diamagnetic Vortices
(a)
(b)
(c)
k=1
2
3
5
10
0.4
0.2
0.0
4
2
0
-2
-25
-50
-75
0.
.1
.2
.3
.4
r
eφ/T
eEr_n/T
r_n^2 ∇^2 eφ/T

Fig. 4.5

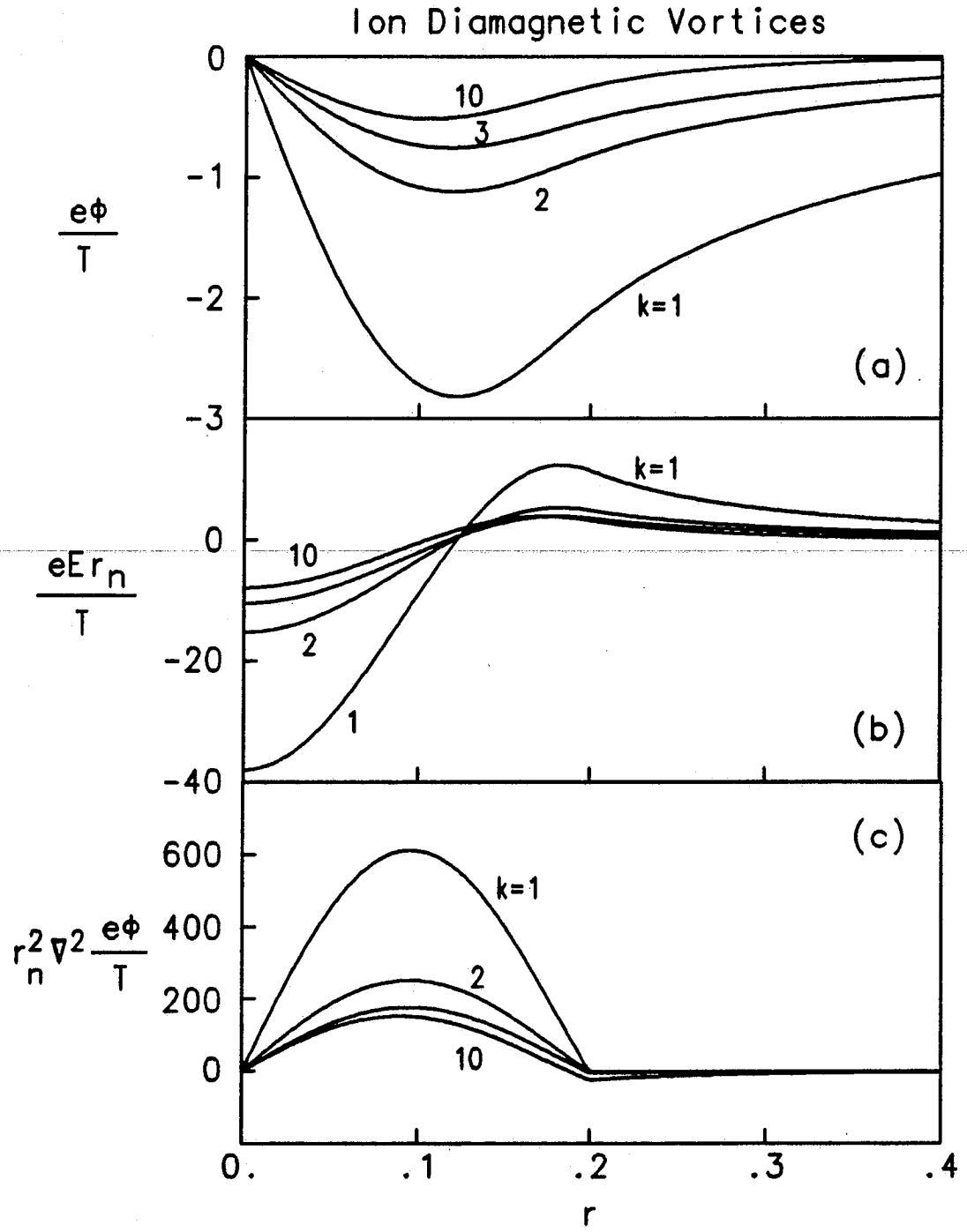
Ion Diamagnetic Vortices
0
-1
-2
-3
eφ/T
10
3
2
k=1
(a)
k=1
0
10
2
-20
1
-40
eEr_n/T
(b)
(c)
600
400
200
0
r_n^2 ∇^2 eφ/T
k=1
2
10
0.
.1
.2
.3
.4
r

Fig. 4.6